

Antiproliferative Effect on Cancer Cells of Novel Pink Red-like Pigments and Derivatives Produced by *Streptomyces coelicoflavus* Strains

Assia Mouslim¹, Saad Menggad², Norddine Habti³, El Bachir Affar², Mohammed Menggad^{1,*}

¹Laboratory of Physiopathology and Molecular Genetics, Faculty of Sciences Ben M'Sik, Hassan II University of Casablanca, Morocco

²MRH Research Center, Department of Medicine, University of Montréal, Canada

³Laboratory of Haematology, Cellular and Genetic Engineering, Faculty of medicine and pharmacy, Hassan II University of Casablanca, Morocco

*Corresponding author: mengm106@yahoo.fr

Received August 19, 2019; Revised September 25, 2019; Accepted October 11, 2019

Abstract Pink red-like pigments of crud extracts produced by *Streptomyces coelicoflavus* MFB11, MFB20, MFB21, MFB23 and MFB24 strains and variants from two spontaneous mutants (MFB11-V and MFB11-Y) as well as prepared fractions (FA and FB) from MFB21 and MFB24 strain pigments were screened for antiproliferative effect by MTT. Cancer cell targets used in this screening were P3 Mice myeloid cell line and/or U2OS human osteosarcoma cell line. The results showed an important antiproliferative effect of some strain pigments on the two organism cell types. U2OS human osteosarcoma cell line was more sensitive to the pigments and showed different antiproliferative effect profiles compared to results obtained on P3 Mice myeloid cell line. FACs analysis of these antiproliferative effects on U2OS human osteosarcoma cell line exhibited cell cycle phase arrests at G1, G1/S or S. This suspects similar mechanism of cell division arrest in U2OS cell induced by these studied compounds to that induced by the apoptotic prodigiosin who differs to that induced by undecylprodigiosin, daunorubicin or other known anthracycline analogues. Thus, these red-like pigments without antibiotic effect unlike prodiginines and anthracyclines could constitute novel related compounds presenting a strong potential for their contribution in anticancer chemotherapy.

Keywords: pigment, anthracycline, antiproliferative, cancer cells, cycle phase arrest, *S. coelicoflavus*

Cite This Article: Mouslim A., Menggad S., Habti N., Affar E. B., and Menggad M., "Antiproliferative Effect on Cancer Cells of Novel Pink Red-like Pigments and Derivatives Produced by *Streptomyces coelicoflavus* Strains." *Journal of Cancer Research and Treatment*, vol. 7, no. 1 (2019): 27-33. doi: 10.12691/jcrt-7-1-5.

1. Introduction

Actinobacteria produce a wide range of pigments which present diverse colors and diverse biological activities [1,2]. These pigments can be diffusible and then secreted in culture media or intracellular non-diffusible [3]. The anthracyclines antibiotics pigments represent the most studied actinobacteria pigments due to their anticancer activities used in chemotherapy [4]. These molecules are classified among the type II family of aromatic polyketides [5]. Their biosynthesis is usually mediated by type II polyketide synthases (PKSs) related to fatty acid synthase (FAS) enzymes [5,6]. Iterative condensation of an acyl-coenzymeA (CoA) starter with malonyl-A extender units by PKSs leads to the aglycone structure. Modifying enzymes act on this polyketide core to create structural diversity of the same compound [7,8,9,10]. Daunorubicin and doxorubicin were the first anthracyclines isolated from the *Streptomyces peucetius* in the 1950s and used in

cancer chemotherapy [11,12,13]. Their analogues Epirubicin, Idarubicin and Valrubicin with more improved efficiency have been developed and further used in cancer treatment [14]. These molecules are known by their high cytotoxicity eliciting apoptosis in cancer cells [15,16]. However, even the extensive use of anthracyclines in clinical treatment of different types of cancer [17,18], their complex mechanism of action still not yet completely understood. Known aspects of this mechanism mostly studied in doxorubicin involve DNA replication and transcription blockage. This blockage is accomplished by intercalating between base pairs of DNA and RNA strands [19] and inhibition of topoisomerase II; causing initiation of DNA damage and induction of apoptosis [20]. Other studies included topoisomerase I inhibition [21], activation of p53 protein-DNA binding [22], induction of cyclin-dependent kinase inhibitor p21(WAF1/CIP1) gene expression, fixation to proteasome which facilitate anthracyclines transport into nucleus where it binds to DNA [23], free radicals generation [20] and Lipid peroxidation [24]. Cells exposed to doxorubicin or its analogue MEN 10755 exhibit cycle

phase arrest at G2 [25,26]. However, doxorubicin treatment of Breast cancer cells had shown to cause increase in p53 activity and decrease of telomerase activity accompanied by G0/G1 phase arrest [27]. p53 induced expression of p21(WAF1/CIP1) gene was reported to trigger G1 arrest [28]. Lüpertz et al found that cytotoxicity, cell cycle and apoptotic cell death in human colon cancer cells treated with doxorubicin are dependent of drug concentration and type of incubation [29]. They noted G2 arrest and G0/G1 phase according to the treatment conditions. Hence, the exact structure of the drug molecule, type of cell target and treatment conditions determine which cycle phase should be blocked.

The tripyrrolic red pigments of prodiginine family are also known to induce apoptosis in many types of cancer cells [30,31]. Similar cell targets such as those of doxorubicin and other targets had been reported. However, in this case, apoptosis could occur in p53 deficient cancer cell lines Jurkat and HL-60 [32]; suggesting an additional p53 and DNA damage independent pathway. Cell cycle was reported to be arrested at G1 phase for prodigiosin [33] and G2/M phase for undecylprodigiosin [34]. However, it seems as mentioned above, that cell cycle phase arrest depends of the cell type used. In fact, human colorectal adenocarcinoma cell line (*HT-29*) treated with prodigiosin were blocked at S phase [35] and non-cancer B and T cells treated with undecylprodigiosin were blocked at G1 phase [36,37].

On the other hand, the efficient anticancer activities of anthracycline molecules are considered as most potent compared to other developed drugs. However, the use of these molecules as anticancer therapeutic drugs provokes cardiac cytotoxicity and induce cancer cell resistance; causing health issue [38]. This concern needs more research efforts to develop derivatives or new molecules with more therapeutic efficiency and reduced side effects. In this study, new pink red-like pigments of five strains and variant pigments of two spontaneous mutants were screened for their antiproliferative activities on mice and/or human cancer cell lines with evaluation of their cell cycle phase arrest.

2. Material and Methods

2.1. Strains, Production and Characteristics of Pigments

Strains MFB11, MFB20, MFB21, MFB23 and MFB24 were isolated from soil and identified as *Streptomyces coelicoflafus* [3,39]. Strains MFB11-V and MFB11-Y with respectively violet and yellow colonies were obtained after repeated culture of strain MFB11. Production of pigments in ISP4 medium and ethanol extraction were performed as previously described [39]. FA and FB fractions of MFB21 and MFB24 strains were prepared from ethanolic crude extracts according to their respective solubilities in petroleum ether and chloroform. Initial ethanolic crude extract of pigment was air dried on watch glass in fume hood till a powdered form of the pigment was obtained. The pigment was then suspended in the petroleum ether to obtain FA fraction and the remaining pigment on watch glass was suspended in chloroform to obtain FB fraction.

UV-Vis spectra and thin-layer chromatography (TLC) analysis on Silica gel G-60 F254 (Merck) were carried out as in as in reference [39]. Solvent systems were: (A) Petroleum ether: Ether (2:1), (B) Ether, (C) Methanol: Ethyl acetate: Chloroform (6:3:1), (D) Chloroform: Methanol (95:5) and (E) chloroform.

2.2. MTT Antiproliferative Assays

Antiproliferative activity of crude extract, FA fraction and FB fraction were tested on P3 Mice myeloid cell line and U2OS human osteosarcoma cell line.

2.2.1. Mice Myeloid Cells

P3 Mice myeloid cell line culture (200 μ l at 4.10^4 cells/ml in RPMI 1640 (Roswell Park Memorial Institute) medium supplemented with 10% of fetal bovine serum was made in 96 well-Microplat and incubated at 37 °C with 5% CO₂. After 3 days incubation, 100 μ l of RPMI supernatant were removed and 100 μ l of fresh RPMI containing pigment to test at desired concentration will DMSO was used as a negative control. After incubation for 3 supplement days, 20 μ l MTT (3-(4,5-dimethylthiazol-2-yl)-2,5-diphenyltetrazolium bromide) at 5 mg/ml in RPMI are added in each well. The plate was incubated for 3 hours and centrifuged at 800 g for 15 min. Supernatant was removed and 100 μ l de DMSO are added in the wells, mixed 30 min and absorbance at 570_{nm} (OD_{570nm}) was determined.

2.2.2. Human Osteosarcoma Cells

U2OS human osteosarcoma cells were cultured in Dulbecco's modified eagle's medium (DMEM) supplemented with 5% of new born serum (NBS), 1% glutamine, 1% of penicillin and 1% of streptomycin. Cells were plated at 20 000 cells density per ml per well in a 24-well plate and left overnight to adhere. Next day, media was changed (1 ml per well) before treatment with the different pigment samples and incubated 72 h. DMSO was used as a negative control and bortezomib as a positive control. Tetrazolium dye MTT was solubilized in DMSO (10 mg/100 μ l) and added to cell culture (1/1000). Cell culture were incubated with added MTT for 3 h at 37°C, washed with PBS-1x before adding Dimethylsulphoxide (DMSO) to each well (200 μ l/well). MTT (yellow product) is reduced by NADPH-dependent cellular oxidoreductase to formazan (purple product). Both products are soluble in DMSO. After shaking, the contents of 24-well plates were transferred to 96-well plate to measure OD_{490 nm}.

2.3. Flow Cytometry (FACs)

Media containing non-adherent cells of the treated cells was transferred from 24-wells plate into fluorescence-activated cell sorting (FACs) tubes. The wells were washed with PBS-1x to transfer the remaining non-adherent cells to FACs tubes. These FACs tubes were centrifuged to get cells in the pellet. The remaining adherent cells in the wells were trypsinised and transferred to the FACs tubes. Total cells were then centrifuged in order to wash them and throw the supernatant. After, cells were suspended in 75% of cold ethanol, vortexed and stored overnight at -20°C. The next day ethanol is aspirated, cells were washed with PBS-1x before being suspended in 500 μ l of

RNase (100 µg/ml PBS-1x) and incubated at 37 °C for 20 min. Finally, 20 µl of propidium iodide (40 µg/ml) were added and vortexed. The mixture was analyzed by using BD Biosciences 2 Laser FacsCalibur Flow Cytometer, and data was processed with FlowJo V887 software.

3. Results

3.1. Spectra and TLC Characteristics

Spectral characteristics and TLC bands obtained with the five mobile phases for MFB11, MFB20, MFB21, MFB23 and MFB24 pigments had been previously reported [39]. Those of MFB11 spontaneous mutants (MFB11-V and MFB11-Y) pigments and fractions (FA and FB) of MFB21 and MFB24 pigments are presented in Table 1 and Table 2). Spectra shapes of MFB11-V violet and MFB11-Y yellow pigments presented modification compared to the parental strain MFB11 pink pigment (Table 1A). In MFB11-V pigment, a λ_{max} at 260 nm has replaced picks at 271 and 491 nm of the parental strain pigment and in MFB11-Y pigment, λ_{max} at 219, 242 and 402 nm were all different of those of the parental strain pigment. On the other hand, FA and FB Fractions of MFB21 and MFB24 strains pigments showed spectral shape modifications compared to those of their respective original crud extract pigment (Table 1B). TLC with solvent A showed net difference between the unique band of MFB11-V violet pigment and that of MFB11 pink pigment where the Rf values were 0.18 and 0.10 respectively (Table 2). With the same solvents, three bands (Rf: 0.34, 0.67 and 0.90) were obtained in the case of MFB11-Y yellow pigment. Moreover, irrespective of

solvent used, this yellow pigment showed mostly yellow bands with different Rf values as indicated in Table 2. Furthermore, analysis of these TLC profiles of the bands numbers and colors obtained according to the solvent used, showed clear differences between MFB11-V, MFB11-Y and MFB11-parent pigments.

On the other hand, even MFB21 and MFB24 pigments presented similar TLC profiles, FA and FB fractions presented differences mostly on the Rf values compared to their crud original pigments of each MFB21 and MFB24 strains. With solvent B, additional yellow band (Rf: 0.96) appeared in FA of the two strains, whereas with solvent D a violet band (Rf: 0.51) emerged in FB of MFB24 pigment. Even similar, TLC profiles of FA of the two strains presented differences on the Rf values mostly with solvent D. Thus, TLC profiles were different between FA and FB fractions of each strain (MFB21, MFB24).

Table 1. UV-Vis spectra picks (λ_{max}) of (A) spontaneous mutants MFB11-V and MFB11-Y pigments compared to their parental strain MFB11 crud extracts and of (B) fractions FA and FB of strains MFB21 and MFB24 compared to their respective initial crud extracts

A		Peaks at	
MFB11		209, 271, 491 and 534 nm	
MFB11-V		205, 260 and 535 nm	
MFB11-Y		219, 242 and 402 nm	
B		Strain	
Extract/Fraction		MFB21	MFB24
Crud Extract		217, 266, 350-352 and 534 nm	211, 266-268 and 534 nm
FA		205, 270, 292 and 534 nm	229 and 533 nm
FB		213, 266 and 534 nm	228, 265 and 530 nm

Table 2. TLC band Rf values and colors of (A) MFB11-V and MFB11-Y spontaneous mutant pigments compared to their MFB11 parental strain crud extract and of (B) FA and FB fractions of MFB21 and MFB24 strains compared to their respective initial crud extracts in different solvent systems

A		Solvent systems				
Strain crud Extract		E	A	B	C	D
MFB11		Pink: 0,26 Pink: 0,56 Pink orange: 0,65 Light yellow: 0,83	Pink: 0,10	Pink: 0,72 Light yellow: 0,95	Pink: 0,61 Pink violet: 0,74	Pink: 0,69 Pink: 0,85
MFB11-V		Pink: 0,06 Pink: 0,53 Pink orange: 0,66 Light yellow: 0,88	Pink: 0,18	Pink: 0,73 Light yellow: 0,96	Light yellow: 0,10 Pink violet: 0,76	Pink: 0,73 Pink: 0,87
MFB11-Y		Yellow: 0,74 Yellow: 0,84	Yellow: 0,34 Yellow: 0,67 Yellow: 0,90	Yellow: 0,95	Yellow: 0,58 orange: 0,74	orange: 0,81 Yellow: 0,85
B		Strain	Extract/Fraction			
MFB21	Crud Extract		Pink: 0,05 Pink: 0,50 Pink orange: 0,63	Pink: 0,12	Pink: 0,77	Pink violet: 0,76 Pink: 0,59 Pink: 0,80
	FA		Pink: 0,02 Pink: 0,33 Pink orange: 0,41	Pink: 0,14	Pink: 0,75 Yellow: 0,96	Pink violet: 0,65 Pink: 0,59 Pink: 0,71
	FB		Pink: 0,02 Pink: 0,3 Pink orange: 0,41	Pink: 0,11	Pink: 0,77	Pink violet: 0,74 Pink: 0,59 Pink: 0,75
MFB24	Crud Extract		Pink: 0,06 Pink: 0,53 Pink orange: 0,65	Pink: 0,12	Pink: 0,71	Pink violet: 0,73 Pink: 0,65 Pink: 0,82
	FA		Pink: 0,04 Pink: 0,34 Pink orange: 0,43	Pink: 0,13	Pink: 0,77 Yellow: 0,96	Pink violet: 0,79 Pink: 0,65 Pink: 0,82
	FB		Pink: 0,02 Pink: 0,31 Pink orange: 0,41	Pink: 0,12	Pink: 0,77	violet: 0,51 Pink: 0,65 Pink: 0,82

3.2. Antiproliferative Activity on Mice Myeloid Cell

Chosen crude extracts and fractions (FA and FB) of the pigments were tested by MTT assay to evaluate their antiproliferative effect on mice P3 myeloid cell line. In these assays, concentrations of material were increased from 5 to 30 $\mu\text{g/ml}$. As shown in Figure 1 at 30 $\mu\text{g/ml}$, the crude pigment extract of MFB21 strain exhibited the highest cytotoxic activity (77.41%) while that of MFB20 strain showed 50.38% of cytotoxicity. That of MFB11 strain showed the lower cytotoxic activity (28.95%). However, increase of pigment concentration leads to increase of the antiproliferative effect as clearly exhibited in the cases of MFB21 and MFB20 strains pigments, indicating a correlation between dose and cytotoxic effect.

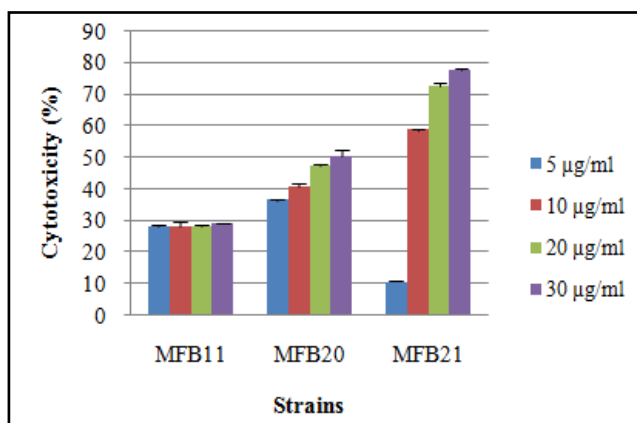


Figure 1. Cytotoxicity effect of crude extract pigments on mice P3 myeloid cancer cell.

Since the crude pigment extract of strain MFB21 showed the highest antiproliferative effect compared to the pigment of the two other used strains, FA and FB fractions of this strain and that of MFB24 (one of non-tested) strain were selected for the following MTT assays. In these next assays, pigment concentrations were started from 30 $\mu\text{g/ml}$. Result showed as for crude extract, increase of fraction concentration leads to increase of the antiproliferative effect (Figure 2).

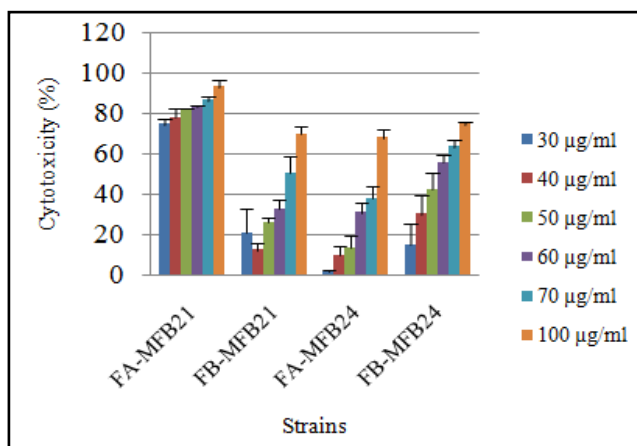


Figure 2. Cytotoxicity effect of FA and FB fractions on mice P3 myeloid cancer cells. Mean values were adjusted with DMSO negative control

At any concentration used, MFB21 FA fraction showed the highest antiproliferative activity. 100 $\mu\text{g/ml}$ of this FA

fraction showed 93.06% cytotoxicity while FB fraction of the same strain showed 70% cytotoxicity. The situation was reversed in MFB24 strain pigment where FA fraction (67,9% at 100 $\mu\text{g/ml}$), showed slight less antiproliferative activity than FB fraction (74,7% at 100 $\mu\text{g/ml}$). Moreover, chloroform soluble MFB21 FB fraction and petroleum ether soluble MFB24 FA fraction showed similar shape of cytotoxicity profiles with any dose and nearly equivalent cytotoxicity at 100 $\mu\text{g/ml}$; respectively 70% and 67,9%. This indicated structural difference between pigments of MFB21 and MFB24 strains leading to antiproliferative differences in their respective FA and FB fractions.

3.3. Antiproliferative Activity on Human Myeloid Cell and Cell Cycle Arrest

After the positive result of MTT antiproliferative assay on mice P3 myeloid cell line, chosen pigment samples were used to evaluate their antiproliferative effect on human U2OS cell line. Cells were treated for 72h with different samples at the most effective concentration of 100 $\mu\text{g/ml}$. The result revealed that the P3 mice cells untested crude extract of MFB23 pink, MFB11-V violet and MFB11-Y yellow pigments exhibited respectively 100%, 99.34% and 54.41% cytotoxicity (Figure 3).

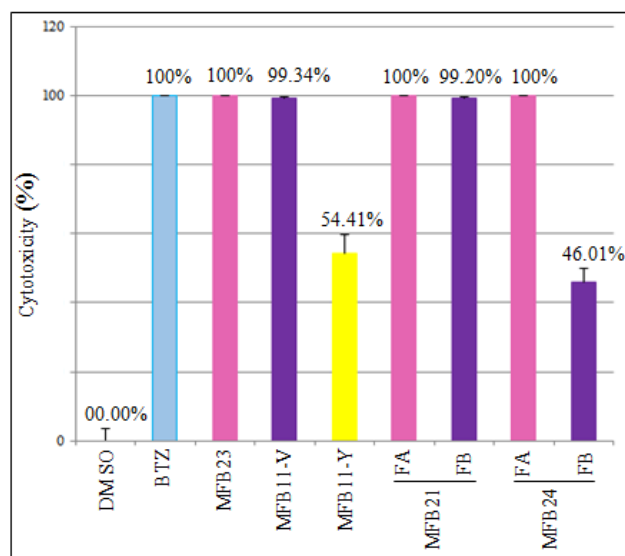


Figure 3. Cytotoxicity effect of MFB23, MFB11-V, MFB11-Y crude extracts and FA/FB fractions of MFB21 and MFB24. DMSO and BTZ were used respectively as negative and positive controls. Mean values were adjusted with DMSO negative control

This result contributed first to affirm that all the strains MFB11, MFB20, MFB21, MFB23 and MFB24 pink pigments exhibited cancer cells antiproliferative effect at different ranges. Dramatic decrease of cell proliferation was obtained by MFB21 FA and FB fractions as well as MFB24 FA fraction (Figure 3) while curiously MFB24 FB fraction exhibited only 46.01% cytotoxicity. Cytotoxicity of MFB21 FA on U2OS cells did not make significant difference to that of MFB21 FB and MFB24 FA compared to that obtained on P3 mice cells. Moreover, MFB24 FB fraction with higher cytotoxicity on P3 mice cells (74.7% at 100 $\mu\text{g/ml}$) than MFB21 FB (70%) and MFB24 FA (67,9%) fractions showed a weak cytotoxicity (46.01%) on U2OS cells (Table 3).

Table 3. Comparison of cytotoxicity percent at 100 µg/ml of fraction A and fraction B of MFB21 and MFB24 strains on P3 myeloid cell line and on U2OS human osteosarcoma cell line

Strain	Cell line	P3		U2OS		
		Fraction	FA	FB	FA	FB
MFB21	MFB21		93.06%	70%	100%	99.20%
	MFB24		67.9%	74.7%	100%	46.01

Flow cytometry analysis was performed in the same conditions as MTT proliferation assay except that cells were treated during 24 h. Negative and positive controls were carried out by using DMSO and bortezomib respectively. The result revealed that pink red-like pigment inhibits the proliferation of U2OS human osteosarcoma cells inducing weak or strong cell cycle arrest in the G1 and/or S phases according to the strain producer and fraction used (Figure 4). Crud extract of MFB11-V causes G1 and S phases arrest whereas those of MFB11-Y and MFB23 cause only G1 phase arrest. In the case of fractions of MFB21, FA causes G1 phase arrest while FB causes S phase arrest. Interestingly FA fraction of MFB24, with similar profile of cytotoxicity on P3 mice cells as MFB21 FB, causes also S phase arrest.

4. Discussion and Conclusion

First, this study indicated that spectral and TLC analysis of violet and yellow crud extract pigments of the MFB11-V and MFB11-Y new mutant as well as FA and

FB fractions of MFB21 and MFB24 strains (Table 1, Table 2) showed characteristics in accordance with previous report [39]. These characteristics were similar to prodiginine family molecules [40,41,42].

On the other hand, the novel pink red-like pigment analogues produced by MFB11, MFB20, MFB21, MFB23 and MFB24 strains inhibit cancer cell proliferation of mice P3 myeloid cell line and/or of human osteosarcoma U2OS cell line (Figure 1, Figure 2, Figure 3) in agreement with cancer cell antiproliferative ability of prodiginine and anthracyclines [11,12,43]. Cell proliferative inhibition profiles were different according to the difference of the pigments produced from the different strains studied and of FA/FB fractions from MFB21 and MFB24 strains. In fact, antiproliferative effect were equivalent as in MFB21 FB/MFB24 FA (Figure 2) or variable and range from weak to strong (100%) as showed by MFB23 crud extract, MFB21 FA and MFB24 FA (Figure 3). MFB21 strain FA fraction was more effective on both P3 mice cell and human U2OS cell types than its FB fraction (Figure 2, Figure 3). However, the situation was inversed in the case of the MFB24 strain where the FB chloroform fraction was more effective than FA petroleum ether fraction on P3 mice cells (Figure 2). This case related independency of antiproliferative activity from compound solvent solubility. Moreover, except the MFB24 FB fraction, MFB21 FA, MFB21 FB and MFB24 FA fractions exhibited higher cytotoxicity on U2OS cells than that obtained on P3 mice cells (Table 3) indicating more sensitivity of human U2OS cells to these compounds.

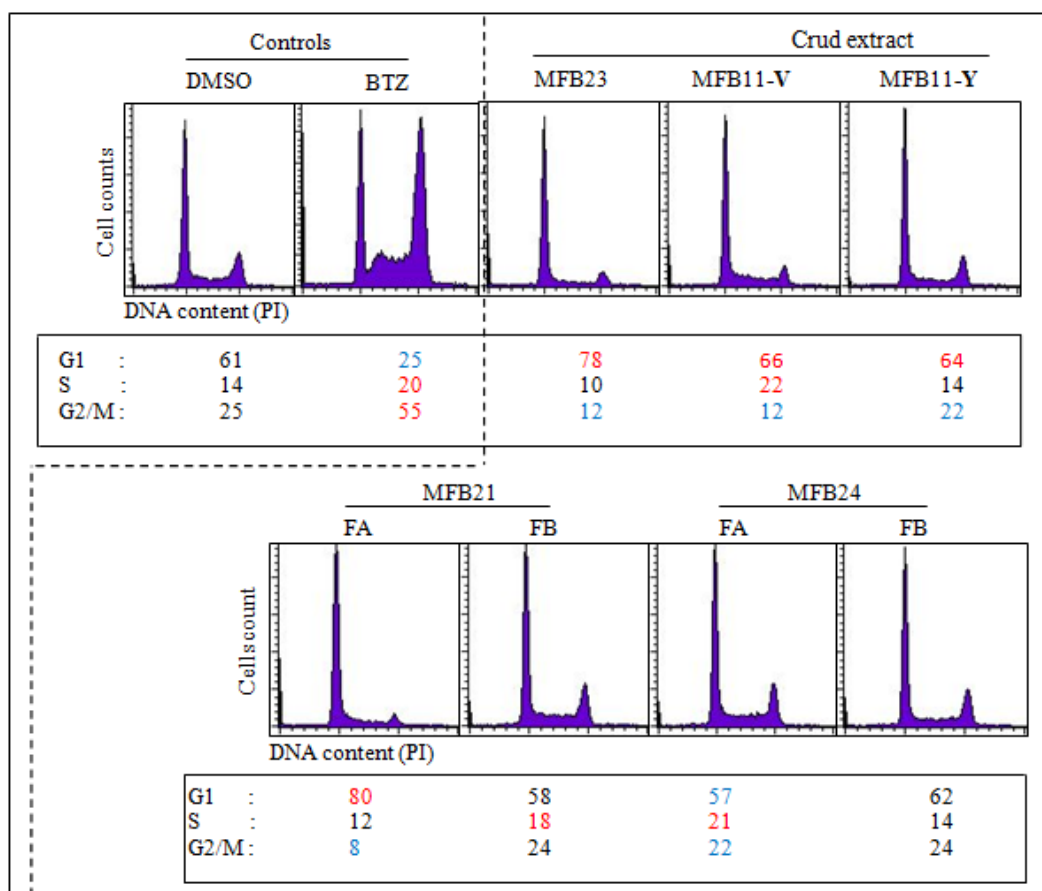


Figure 4. FACS result with cells percent at different cell cycle phases (G1, S and G2/M). (A) Negative (DMSO) and positive (bortezomib) controls, strains MFB23, MFB11-V and MFB11-Y pigments. (B) FA and FB pigment fractions of MFB21 and MFB24 strains. Increased and decreased cells percent compared to negative control (DMSO) are in red or in blue respectively.

Elsewhere, spectral and TLC analysis demonstrated the variability of the MFB11-V violet and MFB11-Y yellow pigment compared to their MFB11 pink parental pigment (Table 1, Table 2) which had a very weak cytotoxicity and dose independent on P3 mice cell (Figure 1). Violet pigment of MFB11-V mutant acquired strong bioactivity against human osteosarcoma U2OS cells than MFB11-Y yellow pigment (Figure 3). Thus, successive culture of these *S. coelicoflafus* strains could generate spontaneous mutants producing structurally variable molecules with more efficiency. The variable antiproliferative bioactivities of these samples reflected different stereochemical structures of the inside compounds which react according to the nature of target cancer cells as exhibited by the studied anthracycline molecules [44].

FACS analysis in this study revealed that, except MFB24 FB with weak cytotoxicity and no cycle phase arrest, the fractions FA and FB cause only G1 or S phase arrest while crud extract could cause G1 and S phases arrest. These postulate the presence of two types of compounds in crud extract of the same strain as MFB11-V causing G1 and S phases arrest or one type of compound as in MFB23 causing only G1 phase arrest. In the fractions, the compounds seem to be separated in FA and FB causing only arrest at G1 phase or S phase. These results suggest the presence of two mechanisms triggered by these compounds in cell cycle phase arrest. As induced by the apoptotic prodigiosin, the first mechanism leads to G1 phase arrest on human Jurkat leukaemia T cell [33] and a second leads to S phase arrest on HT-29 human colorectal adenocarcinoma cell line [35]. However, bortezomib used as a positive control is known to induce G2/M cell phase arrest and apoptosis. Longer treatment time with bortezomib creates a sub-G1 peak characteristic of cell population apoptosis [45]. Thus, treatment time should be longer to investigate if apoptosis follows G1 arrest created by MFB21 FA fraction and MFB23 crud extract. Equally, this allow to investigate if the weak accumulation of cells in S phase after treatment with MFB21 FB and MFB24 FA fractions will increase and lead to apoptosis.

In conclusion, this study provided a polymorphic stock of pink red-like pigments and derivatives with strong or weak antiproliferative activities causing cell cycle arrest at G1 and/or S phase. These pigments, even related to the apoptotic prodigiosin, constitute novel compound analogues. The stock could be increased with creating more polymorphic molecules as demonstrated by spontaneous mutations. Nevertheless, more detailed investigations including purification and chemical structure of these compounds, combined with their efficiencies on other human cancer cell lines and their side effects, are needed for their fundamental or clinical contribution in cancer chemotherapy.

References

- [1] Soliev A B, Hosokawa K and Enomoto K, Bioactive Pigments from Marine Bacteria: Applications and Physiological Roles, *Evidence-Based Complementary and Alternative Medicine, eCAM*, 2011, 670349.
- [2] Conn H J, Conn J E, Value of Pigmentation in Classifying Actinomycetes: A Preliminary Note. *J Bacteriol*, 42 (6). 791-799. Dec 1941.
- [3] Ayoubi H, Mouslim A, Moujabbir S, Amine S, Azougar I, Mouslim J and Menggad M, Isolation and phenotypic characterization of actinomycetes from Rabat neighborhood soil and their potential to produce bioactive compounds, *Afr J Microbiol Res*, 12 (8). 186-191. Feb 2018.
- [4] Nadas J and Sun D Anthracyclines as effective anticancer drugs. *Expert Opin Drug Discov*, 1 (6). 549-68. Nov 2006.
- [5] Zhang Z, Gong YK, Zhou Q, Hu Y, Ma HM, Chen YS, Igarashi Y, Pan L and Tang GL, Hydroxyl regioisomerization of anthracycline catalyzed by a four-enzyme cascade, *Proc Natl Acad Sci*, 114 (7). 1554-1559. Feb 2017.
- [6] Das A and Khosla C, Biosynthesis of aromatic polyketides in bacteria, *Acc Chem Res*, 42 (5). 631-9. Mar 2009.
- [7] Khosla C, Gokhale R S, Jacobsen J R and Cane D E, Tolerance and specificity of polyketide synthases, *Annu Rev Biochem*, 68. 219-253. Jul 1999.
- [8] Bartel PL, Connors NC and Strohl WR, Biosynthesis of anthracyclines: analysis of mutants of *Streptomyces* sp. strain C5 blocked in daunomycin biosynthesis, *J Gen Microbiol*, 136. 1877-1886. Jun 1990.
- [9] Connors NC, Bartel PL and Strohl WR, Biosynthesis of anthracyclines: enzymatic conversion of aklanonic acid to aklavinone and ϵ -rhodomycinone by anthracycline-producing streptomycetes, *J Gen Microbiol*, 136. 1887-1894. May 1990.
- [10] Eckardt K and Wagner C, Biosynthesis of anthracyclines, *J Basic Microbiol*, 28 (1-2). 137-144. 1988.
- [11] Coombs C C, Tavakkoli M and Tallman M S, Acute promyelocytic leukemia: where did we start, where are we now, and the future, *Blood Cancer Journal*, 2015 Apr 17, 5(4): e304.
- [12] Arcamone F, Antitumor anthracyclines: recent developments. *Med Res Rev*, 4 (2). 153-188. Apr-Jun 1984.
- [13] Grein A, Spalla C, di Marco A, and Canevazzi G, "Descrizione e classificazione di un attinomicete (*Streptomyces peucetius* sp. nova). Produttore di una sostanza ad attivit antitumorale: la daunomicina", *Giorn Microbiol*, 11. 109-118. (Italian). (1963).
- [14] Minotti G, Menna P, Salvatorelli E, Cairo G and Gianni L, Anthracyclines: Molecular Advances and Pharmacologic Developments in Antitumor Activity and Cardiotoxicity, *Pharmacol Rev*, 56 (2). 185-229. Jun 2004.
- [15] Dartsch DC, Schaefer A, Boldt S, Kolch W and Marquardt H, Comparison of anthracycline-induced death of human leukemia cells: Programmed cell death versus necrosis, *Apoptosis*, 7 (6). 537-548. Dec 2002.
- [16] Ferraro C, Quemeneur L, Prigent AF, Taverne C, Revillard JP, et al. Anthracyclines trigger apoptosis of both G0-G1 and cycling peripheral blood lymphocytes and induce massive deletion of mature T and B cells, *Cancer Res*, 60 (7). 1901-1907. Dec 2000.
- [17] Mort MK, Sen JM, Morris AL, DeGregory KA, McLoughlin EM, Mort JF, Dunn SP, Abuannadi M and Keng MK, Evaluation of cardiomyopathy in acute myeloid leukemia patients treated with anthracyclines, *J Oncol Pharm Pract*, 2019 Sep 9: 1078155219873014.
- [18] Khan MA, D'Ovidio A, Tran H and Palaniyar N, Anthracyclines Suppress Both NADPH Oxidase-Dependent and -Independent NETosis in Human Neutrophils, *Cancers*, 2019, 11 (9).
- [19] Wang AHJ, Intercalative drug binding to DNA, *Curr Opin Struct Biol*, 2 (3). 361-368. Jun 1992.
- [20] Gewirtz DA, A critical evaluation of the mechanisms of action proposed for the antitumor effects of the anthracycline antibiotics adriamycin and daunorubicin, *Biochem Pharmacol*, 57 (7). 727-741. Apr 1999.
- [21] Guano F, Pourquier P, Tinelli S, Binaschi M, Bigioni M, Animati F, Manzini S, Zunino F, Kohlhagen G, Pommier Y and Capranico G. Topoisomerase poisoning activity of novel disaccharide anthracyclines, *Mol Pharmacol*, 56 (1). 77-84. Jul 1999.
- [22] Bertheau P, Plassa F, Espie M, Turpin E, de Roquancourt A, Marty M, Lerebours F, Beuzard Y, Janin A, and de The H, Effect of mutated TP53 on response of advanced breast cancers to high-dose chemotherapy, *Lancet*, 360 (9336). 852-854. Sep 2002.
- [23] Kiyomiya K, Matsuo S, and Kurebe M, Mechanism of specific nuclear transport of adriamycin: the mode of nuclear translocation of adriamycin-proteasome complex, *Cancer Res*, 61 (6). 2467-2471. Apr 2001.
- [24] Plastaras JP, Dedon PC, and Marnett LJ, Effects of DNA structure on oxopropenylation by the endogenous mutagens malondialdehyde and base propenal, *Biochemistry*, 41 (16). 5033-5042. Apr 2002.

- [25] Bigioni M, Salvatore C, Bullo A, Bellarosa D, Iafrate E, Animati F, Capranico G, Goso C, Maggi CA, Pratesi G, et al. A comparative study of cellular and molecular pharmacology of doxorubicin and MEN 10755, a disaccharide analogue, *Biochem Pharmacol*, 62 (1): 63-70. Jul 2001.
- [26] Ling Y H, el-Naggar A K, Priebe W and Perez-Soler R, Cell cycle-dependent cytotoxicity, G2/M phase arrest, and disruption of p34cdc2/cyclin B1 activity induced by doxorubicin in synchronized P388 cells, *Molecular Pharmacology*, 49 (5). 832-841. May 1996.
- [27] Elmore LW, Rehder CW, Di X, McChesney PA, Jackson-Cook CK, Gewirtz DA and Holt SE, Adriamycin-induced senescence in breast tumor cells involves functional p53 and telomere dysfunction; *J Biol Chem*, 277 (38): 35509-35515. Oct 2002.
- [28] Zhang W, Kornblau SM, Kobayashi T, Gambel A, Claxton D and Deisseroth AB, High levels of constitutive WAF1/Cip1 protein are associated with chemoresistance in acute myelogenous leukemia, *Clin Cancer Res*, 1 (9). 1051-1057. Sep 1995.
- [29] Lüpertz R, Wätjen W, Kahl R and Chovolou Y, Dose- and time-dependent effects of doxorubicin on cytotoxicity, cell cycle and apoptotic cell death in human colon cancer cells, *Toxicology*, 271 (3). 115-21. May 2010.
- [30] Chang CC, Chen WC, Ho SF, Wu HS and Wei YH, Development of natural anti-tumor drugs by microorganisms, *J Biosci Bioeng*, 111 (5). 501-511. May 2011.
- [31] Williamson NR, Fineran PC, Gristwood T, Chawrai SR, Leeper FJ, Salmond GPC Anticancer and immunosuppressive properties of bacterial prodiginines, *Future Microbiol*, 2 (6). 605-618. Dec 2007.
- [32] Vogelstein B, Lane D and Levine AJ, Surfing the p53 network, *Nature*, 408 (6810). 307-10. Nov 2000.
- [33] Perez-Tomas R and Montaner B. Effects of the proapoptotic drug prodigiosin on cell cycle-related proteins in Jurkat T cells. *Histol Histopathol*. 18 (2003): 379-85.
- [34] Liu P, Wang Y, Qi X, Gu Q, Geng M, Li J. Undecylprodigiosin Induced Apoptosis in P388 Cancer Cells Is Associated with Its Binding to Ribosome. St-Pierre Y, ed. *PLoS ONE*. 8 (2013): e65381.
- [35] Dalili D, Fouladdel Sh, Rastkari N, Samadi N, Ahmadvaniha R, Ardavan A and Azizi E, Prodigiosin, the red pigment of *Serratia marcescens*, shows cytotoxic effects and apoptosis induction in HT-29 and T47D cancer cell lines, *Natural Product Research*, 26 (22). 2078-2083. 2012.
- [36] Mortellaro A, Songia S, Gnocchi P, Ferrari M, Fornasiero C, D'Alessio R, Isetta A, Colotta F and Golay J, New immunosuppressive drug PNU156804 blocks IL-2-dependent proliferation and NF-kappa B and AP-1 activation, *J Immunol*, 162 (12). 7102-7109. Jul 1999.
- [37] Songia S, Mortellaro A, Taverna S, Fornasiero C, Scheiber EA, Erba E, Colotta F, Mantovani A, Isetta AM, Golay J, Characterization of the new immunosuppressive drug undecylprodigiosin in human lymphocytes: retinoblastoma protein, cyclin-dependent kinase-2, and cyclin-dependent kinase-4 as molecular targets, *J Immunol*, 158 (8). 3987-95. Apr 1997.
- [38] Myers C E, Mimnaugh E G, Yeh G C and Sinha B K, Biochemical mechanisms of tumor cell kill by anthracyclines. In *Anthracycline and Anthracenedione-Based Anti-Cancer Agents*, pp. 527-569. Edited by J. W. Lown. Amsterdam: Elsevier. (1988).
- [39] Mouslim A, Ayoubi H, Moujabbir S, Mouslim J and Menggad M, Physico-chemical Characterization of a Pink Red-like Pigments Produced by Five New Bacterial Soil Strains Identified as *Streptomyces coelicoflavus*, *Am J Microbiol Res*, 6 (3). 67-72. Jun 2018.
- [40] Holkar S, Begde D, Nashikkar N, Kadam T and Upadhyay A, Rhodomycin analogues from *Streptomyces purpurascens*: isolation, characterization and biological activities, *SpringerPlus*, 2(1). 93. (13p). Mar 2013.
- [41] Rudd BA and Hopwood DA, A Pigmented Mycelial Antibiotic in *Streptomyces coelicolor*: Control by a Chromosomal Gene Cluster. *Journal of General Microbiology*, 119 (2). 333-340. Aug 1980.
- [42] Williams RP, Green JA and Rappoport DA, Studies on pigmentation of *Serratia marcescens*. I. spectral and paper chromatographic properties of Prodigiosin, *J Bacteriol*, 71 (1). 115-120. Jan 1956.
- [43] Elahian F, Moghimi B, Dinmohammadi F, Ghamghami M, Hamidi M and Mirzaei S A, The Anticancer Agent Prodigiosin Is Not a Multidrug Resistance Protein Substrate, *DNA and Cell Biology*, 32 (3). 90-97. Mar 2013.
- [44] Faheem AR, Anthracyclines: Mechanism of Action, Classification, Pharmacokinetics and Future - A Mini Review, *Int J Biotech & Bioeng*, 4 (4). 81-85. Apr 2018.
- [45] Bonvini P, Zorzi E, Basso G and Rosolen A, Bortezomib-mediated 26S proteasome inhibition causes cell-cycle arrest and induces apoptosis in CD-30⁺ anaplastic large cell lymphoma, *Leukemia*, 21 (4). 838-842. Apr 2007.

